Nonequilibrium phase transition in an Ising model without detailed balance

Manoj Kumar[1,2,*] and Chandan Dasgupta[2,3,†]

[1]*Centre for Fluid and Complex Systems, Coventry University, Coventry CV1 5FB, United Kingdom*

[2]*International Centre for Theoretical Sciences, Tata Institute of Fundamental Research, Bengaluru 560089, India*

[3]*Department of Physics, Indian Institute of Science, Bengaluru 560012, India*

(Received 27 July 2020; accepted 21 October 2020; published 9 November 2020)

We study a two-dimensional ferromagnetic Ising model in which spins are updated using modified versions of the Metropolis and Glauber algorithms. These update rules do not obey the detailed balance condition. The steady-state behavior of the model is studied using molecular field theory and Monte Carlo simulations. This model is found to exhibit a nonequilibrium phase transition from a "paramagnetic" state with zero magnetization to a "ferromagnetic" state with nonzero magnetization as the variable that plays the role of temperature in the spin updates is decreased. From detailed Monte Carlo simulations using the modified Metropolis algorithm, we demonstrate explicitly the nonequilibrium nature of the transition and show that it cannot be described as an equilibrium transition with an effective temperature different from the temperature used in the spin updates. The critical exponents that characterize the singular behavior near this continuous phase transition are calculated from finite size scaling of specific heat, magnetization, susceptibility, and correlation length. We find that the values of these exponents are the same (within error bars) as those of the equilibrium Ising model in two dimensions.

DOI: 10.1103/PhysRevE.102.052111

I. INTRODUCTION

The critical behavior near continuous phase transitions in systems in equilibrium is fairly well understood at present [1]. A similar understanding is not available for phase transitions in nonequilibrium systems [2–5]. Nonequilibrium phase transitions are found in a wide variety of systems. These include driven diffusive systems [6–18], kinetic Ising models with competing dynamics [19–28], stochastic models of driven interfaces and growing surfaces [29–32], reaction-diffusion models [5,13,33–36], and models of depinning transition [37].

In recent years, a lot of attention has been focused on studies of collective properties of "active" systems [38] consisting of self-propelled objects that generate systematic motion from internal or ambient sources of energy. Some of these out-of-equilibrium systems exhibit interesting phase transitions [39–41]. For example, many active systems exhibit motility induced phase separation [41] in which the system spontaneously breaks up into a dilute, gaslike phase and a dense liquidlike phase even if there is no attractive interaction between the particles. The liquid-gas phase boundary exhibits a critical point similar to the equilibrium liquid-gas critical point that is known to be in the Ising universality class. Other Ising-like critical points are found in systems with scalar activity, consisting of two kinds of particles with different temperatures [42–44] or diffusivities [45]. Some of these systems [42,43,45] exhibit phase separation and a critical point similar to the liquid-gas critical point in equilibrium systems. These phase transitions are not completely understood. There have been a few numerical investigations [43,46,47] of the critical behavior near the critical point in these systems. While two of these studies [43,46] suggest that the critical point belongs in the Ising universality class, the third one [47] concludes that the universality class is different from that of the equilibrium Ising model.

Further, a rich variety of critical behavior has been observed in nonequilibrium Potts-like models with q absorbing states [48–50] in which the nature of phase transitions depends on the value of q and the dimension d. In these studies, the absorbing states are obtained by imposing a restriction in the dynamics that no spin flips are allowed when all neighbors of a given spin are in the same state as that of the given spin. Such models in $d = 1$ with a single absorbing state ($q = 1$) [34,51] or with infinitely many absorbing states [52,53] are known to lie in the universality class of directed percolation (DP) [33,37,54]. While in $d = 2$, these models with two symmetric absorbing states ($q = 2$) are shown to belong to a new universality class called a voter universality class [49,50]. Moreover, for an extended range of interactions, the critical point has been shown in [48] to split into Ising and DP universality classes. Additionally, a change of symmetry among different absorbing states is also known for altering the universality class [55–57]. Thus it has become clear that there is a diversity in the universality classes of out-of-equilibrium systems and so the problem of classifying nonequilibrium phase transitions is far from complete [5].

In this paper, we consider the phase transition in a two-dimensional Ising-like model in which "activity" is incorporated by changing the rules of updating the spin variables. Ising spins do not have any intrinsic dynamics. The time evolution of Ising spins is often modeled by Monte Carlo dynamics with the Metropolis algorithm [58] that satisfies the

*manoj.kumar@icts.res.in

†chandan.dasgupta@icts.res.in

detailed balance condition (DBC) and is therefore guaranteed to generate spin configurations distributed according to equilibrium Boltzmann probabilities. In the model considered here, "activity" is introduced by modifying the update rules in a way that makes the probability of occurrence of spin flips higher than that in the equilibrium Ising model. These update rules do not satisfy the DBC. Hence the spin configurations in the steady state of this model are not distributed with equilibrium Boltzmann probabilities. The opposite case in which spin flips are less likely to occur than in the equilibrium model is also considered. We call this model a "persistent Ising model" because the update rule tends to increase the persistence time of spin configurations.

We have studied the steady-state properties of this nonequilibrium Ising model using molecular field theory and Monte Carlo simulations. We find that this system exhibits a phase transition between paramagnetic (zero spontaneous magnetization) and ferromagnetic (finite spontaneous magnetization) phases as a temperaturelike variable is changed. While molecular field theory predicts certain unusual phase behavior, our Monte Carlo simulation using a modified version of the Metropolis algorithm shows that this model exhibits a continuous phase transition. The critical behavior near this phase transition is studied using finite-size scaling. Within the accuracy of our calculations, the critical exponents are found to have the same values as those in the ferromagnetic Ising model in two dimensions.

The rest of the paper is organized as follows. The model considered in our study is introduced and the details of our Monte Carlo simulations are described in Sec. II. In Sec. III, we present analytical arguments for the occurrence of a nonequilibrium phase transition in this model. Section IV describes the phase diagram of this model in the molecular field approximation. In Sec. V, we present detailed numerical results of our simulations and investigate the critical behavior of the model. Finally, in Sec. VI, we conclude with a summary of the main results and discussion.

II. MODEL AND METHODS

The two-dimensional ferromagnetic Ising model with nearest-neighbor interactions is described by the Hamiltonian

$$\mathcal{H} = -J \sum_{\langle ij \rangle} s_i s_j, \tag{1}$$

where $\langle ij \rangle$ represents nearest-neighbor sites on a square lattice and $\{s_i\}$, $i = 1, \ldots, N$ are Ising spins taking the values ± 1. The system is placed in a contact with a heat bath that generates stochastic spin flips [59]. In the equilibrium Ising model, the probabilities of spin flips are chosen such that the system reaches thermal equilibrium after a sufficiently long time and the distribution in the steady state is given by the Boltzmann distribution. The Metropolis [58] and Glauber or heat bath algorithms [60,61] are the two most common choices of the transition rates, given respectively as

$$W = \min[1, \exp(-\beta \Delta E)] \tag{2}$$

and

$$W = \frac{1}{2}\left[1 - \tanh\left(\frac{\beta \Delta E}{2}\right)\right] = \frac{1}{1 + \exp(\beta \Delta E)}, \tag{3}$$

where W is a rate of transition from an old state to a new one, $\Delta E = E_{\text{new}} - E_{\text{old}}$ is the change in energy due to this transition, and $\beta = 1/k_B T$. These algorithms satisfy the *detailed balance condition* (DBC) which implies microscopic reversibility [62] with each elementary process balanced with its reverse process, i.e.,

$$W_{\text{old}\to\text{new}} P_{\text{eq}}(\text{old}) = W_{\text{new}\to\text{old}} P_{\text{eq}}(\text{new}), \tag{4}$$

where $P_{\text{eq}}(\text{old}) \propto \exp(-\beta E_{\text{old}})$, and therefore

$$\frac{W_{\text{old}\to\text{new}}}{W_{\text{new}\to\text{old}}} = \exp(-\beta \Delta E). \tag{5}$$

The DBC is a sufficient—but not necessary—condition to ensure equilibration [4]. In this paper, our motive is to intentionally break the DBC in a way that causes the system to go out of equilibrium and to study whether or not the system exhibits an order-disorder transition. If it does, then is the transition different from the equilibrium phase transition or equivalently do the critical exponents differ from the equilibrium ones? The DBC is violated when ΔE in the transition probabilities is replaced by ΔE_{eff} defined as

$$\Delta E_{\text{eff}} = \Delta E + E_0, \tag{6}$$

where E_0 a nonzero parameter. Then, for $E_0 > 0$, $\Delta E_{\text{eff}} > \Delta E$ and it becomes less probable for spins to flip. Similarly, for $E_0 < 0$, ΔE_{eff} is lower than ΔE and that promotes the flipping of spins. Therefore, in this way the active and persistent limits can be modeled in an Ising system. Spins under these flipping rates effectively experience different temperatures compared to spins with the original Metropolis or Glauber rates. For $E_0 > 0$ ($E_0 < 0$), the spins may be thought of as being coupled to a thermal bath at a lower (higher) effective temperature and the effective temperature is not the same for all the spins in the system (see below). Hence the system is not in equilibrium and a phase transition, if it occurs, is a nonequilibrium one. This transition would be a property of the *nonequilibrium steady state* of the system in which the distribution of microstates is not described by the Boltzmann distribution. We continue to call T the "temperature" in spite of the fact that the temperature is not a well-defined quantity in a nonequilibrium system.

We perform a Monte Carlo (MC) simulation of a two-dimensional Ising model using the modified Metropolis rule. The simulations are done on a square lattice of linear size L with periodic boundary condition applied in both directions. The total number of spins in the system is $N = L^2$. We discard the first 10^5 Monte Carlo steps per spin (MCS) to obtain a *nonequilibrium steady state* of the system, and then perform another 10^5 MCS for measuring averaged quantities. We average all measured quantities over 100 realizations of different random initial conditions and determine the error bars in a quantity from its fluctuations over different realizations. To perform a finite-size scaling (FSS), we use a python program

named *autoscale.py*, developed by Melchert [63]. This program uses a minimization procedure to optimize the scaling parameters via a downhill simplex algorithm [64].

III. OCCURRENCE OF A PHASE TRANSITION

In the modified Metropolis algorithm considered here, the transition rate for flipping a spin $s_i \to -s_i$ is

$$W_{s_i\to -s_i} = \begin{cases} e^{-\beta(\Delta E+E_0)}, & \text{if } \Delta E + E_0 > 0, \\ 1, & \text{otherwise,} \end{cases} \tag{7}$$

where

$$\Delta E = 2Js_i \sum_{n_i} s_{n_i}. \tag{8}$$

Here n_i refers to the nearest neighbors of the ith site. Similarly, the transition rate for flipping spins $-s_i \to +s_i$ is

$$W_{-s_i\to s_i} = \begin{cases} e^{-\beta(-\Delta E+E_0)}, & \text{if } -\Delta E + E_0 > 0, \\ 1, & \text{otherwise.} \end{cases} \tag{9}$$

It is straightforward to check that this algorithm [Eq. (7)] satisfies the DBC only for $E_0 \geqslant \Delta E_{\max}$ and $E_0 \leqslant -\Delta E_{\max}$, where $\Delta E_{\max} = 2zJ$ (z is the number of nearest neighbors of a spin) is the largest possible value of ΔE. This can be explained as follows. Consider first $E_0 \geqslant \Delta E_{\max}$ meaning that $\pm\Delta E + E_0 \geqslant 0$. Therefore, the transition rates are

$$W_{s_i\to -s_i} = e^{-\beta(\Delta E+E_0)}, \quad W_{-s_i\to s_i} = e^{-\beta(-\Delta E+E_0)}, \tag{10}$$

and thus the ratio

$$\frac{W_{s_i\to -s_i}}{W_{-s_i\to s_i}} = \exp(-2\beta\Delta E). \tag{11}$$

Hence DBC is satisfied, *albeit* at an effective temperature $T_{\text{eff}} = T/2$ and, therefore, the critical temperature at which an *equilibrium* transition takes place is given by

$$T_c(E_0 \geqslant \Delta E_{\max}) = 2T_c^0, \tag{12}$$

where $T_c^0 = T_c(E_0 = 0)$ is the critical temperature of the nearest-neighbor Ising model on a square lattice.

For $E_0 \leqslant -\Delta E_{\max}$, $\pm\Delta E + E_0 \leqslant 0$, which implies that $W_{s_i\to -s_i} = W_{-s_i\to s_i} = 1$, and thus the ratio

$$\frac{W_{s_i\to -s_i}}{W_{-s_i\to s_i}} = 1. \tag{13}$$

Therefore, in this case, DBC is satisfied in the limit of $T_{\text{eff}} \to \infty$, implying that the system is effectively at an infinite temperature for all T and there is no phase transition.

For $|E_0| < \Delta E_{\max}$, the DBC is not satisfied because it is not possible to find a unique effective temperature for which the transition probabilities for all possible values of ΔE satisfy detailed balance. This can be shown as follows. First, let us consider $0 < E_0 < \Delta E_{\max}$. Then for $\Delta E > 0$, $W_{s_i\to -s_i} = e^{-\beta(\Delta E+E_0)}$ and $W_{-s_i\to s_i} = \min[1, e^{-\beta(-\Delta E+E_0)}]$; and for $\Delta E < 0$, $W_{s_i\to -s_i} = \min[1, e^{-\beta(\Delta E+E_0)}]$ and $W_{-s_i\to s_i} = e^{-\beta(-\Delta E+E_0)}$. In both cases, the ratio of the transition probabilities will depend upon the value of ΔE and, therefore, it is not possible to define a unique effective temperature. If a phase transition takes place in the system, then the transition temperature T_c should satisfy $T_c^0 < T_c < 2T_c^0$. Similarly, following the same arguments for $-\Delta E_{\max} < E_0 < 0$, it can be shown that T_c should lie in the interval $(0, T_c^0)$. To sum up, $T_c = 0$ for $E_0 \leqslant -\Delta E_{\max}$, it increases from 0 as E_0 is increased from $-\Delta E_{\max}$ to $+\Delta E_{\max}$, and becomes $2T_c^0$ for $E_0 \geqslant \Delta E_{\max}$.

For the Glauber algorithm, the ratio of two transition rates is

$$\frac{W_{s_i\to -s_i}}{W_{-s_i\to s_i}} = \frac{1 + e^{\beta(-\Delta E+E_0)}}{1 + e^{\beta(\Delta E+E_0)}}. \tag{14}$$

Notice that here the DBC is satisfied only in the limit of E_0 approaching $\pm\infty$. For $E_0 \to +\infty$,

$$\frac{W_{s_i\to -s_i}}{W_{-s_i\to s_i}} = \frac{e^{-\beta E_0} + e^{-\beta\Delta E}}{e^{-\beta E_0} + e^{\beta\Delta E}} \to e^{-2\beta\Delta E}, \tag{15}$$

and for $E_0 \to -\infty$,

$$\frac{W_{s_i\to -s_i}}{W_{-s_i\to s_i}} \to 1. \tag{16}$$

For any finite value of E_0 the DBC is not satisfied. The T_c is expected to increase (decrease) with increasing (decreasing) E_0. For a positive finite value of E_0, T_c lies in the interval $(T_c^0, 2T_c^0)$ and approaches $2T_c^0$ in the limit of $E_0 \to \infty$. For $E_0 < 0$, $T_c \in (0, T_c^0)$, and it approaches zero as $E_0 \to -\infty$.

IV. MOLECULAR FIELD THEORY

In molecular field (MF) theory, a spin is replaced by its mean value, i.e., the magnetization m. So Eq. (8) in this approximation is

$$\Delta E = 2Jzms_i, \tag{17}$$

where $z = 2d$ is the number of neighbors in a hypercubic lattice in d dimensions. Thus, in the MF approximation, each spin interacts with the net internal field arising from its interaction with all the neighboring spins.

Using Eq. (17) for ΔE in Eq. (7), the transition rate for Metropolis dynamics in the MF approximation becomes

$$W_{s_i\to -s_i} = \begin{cases} e^{-\beta[2zJms_i+E_0]}, & 2zJms_i + E_0 > 0, \\ 1, & 2zJms_i + E_0 \leqslant 0. \end{cases} \tag{18}$$

We will now construct a self-consistent equation for the magnetizations m under this MF approximation, and then solve it numerically. If a site i has $s_i = +1$, then $W_{+1\to -1}$ in above equation (18) gives the probability of it flipping to $s_i = -1$ and, similarly, $W_{-1\to +1}$ gives the probability of flipping from $s_i = -1$ to $s_i = +1$. Let $p(+1)$ $[p(-1)]$ be the probability of s_i being in the $+1$ (-1) state in the steady state of the system. The ratio of these probabilities is given by

$$\frac{p(-1)}{p(+1)} = \frac{W_{+1\to -1}}{W_{-1\to +1}} \equiv r(\beta, m, E_0), \tag{19}$$

where r defines the probabilities ratio, which is a function of parameters β, m, and E_0.

Then the magnetization m in terms of r is

$$m = \frac{\sum_{s_i=\pm 1} p(s_i)s_i}{\sum_{s_i=\pm 1} p(s_i)} = \frac{1 - r(\beta, m, E_0)}{1 + r(\beta, m, E_0)}. \tag{20}$$

This is a self-consistency equation, which can be solved easily for a few special values of E_0 for which the DBC is

satisfied. In the case of equilibrium dynamics with $E_0 = 0$, $r(\beta, m, E_0 = 0) = e^{-2\beta zJm}$. Consequently,

$$m(E_0 = 0) = \frac{1 - e^{-2\beta zJm}}{1 + e^{-2\beta zJm}} = \tanh[\beta zJm], \tag{21}$$

which is the well-known self-consistency equation for the magnetization of the equilibrium Ising model in MF theory. For $E_0 \geqslant 2zJ$, $2zJms_i + E_0$ is always nonnegative and the ratio $r(\beta, m, E_0) = e^{-4\beta zJm}$. Therefore, from Eq. (20) the MF magnetization satisfies the self-consistency condition

$$m(E_0 \geqslant 2zJ) = \tanh[2\beta zJm]. \tag{22}$$

This is the same as the self-consistency equation for m in the equilibrium Ising model at temperature $T/2$. For $E_0 \leqslant -2zJ$, $2zJms_i + E_0$ is always nonpositive. Hence $r(\beta, m, E_0) = 1$ and therefore $m = 0$.

For positive values of E_0 in the range $0 < E_0 < 2zJ$, the transition probabilities given in Eq. (18) take the following forms for $m \geqslant 0$:

$$W_{+1\to-1} = e^{-\beta[2zJm+E_0]}, \tag{23}$$

$$W_{-1\to+1} = \begin{cases} e^{-\beta[-2Jzm+E_0]}, & -2zJm + E_0 > 0, \\ 1, & -2zJm + E_0 \leqslant 0. \end{cases} \tag{24}$$

Then, for $2zJm > E_0$, $W_{-1\to+1} = 1$. This gives the following self-consistency equation for m:

$$m(2zJm > E_0) = \tanh[\beta(Jzm + E_0/2)]. \tag{25}$$

On the other hand, using $W_{-1\to+1} = \exp[-\beta(-2zJm + E_0)]$ for $2Jzm < E_0$ will give

$$m(2zJm < E_0) = \tanh(2\beta Jzm), \tag{26}$$

which is identical to the self-consistency equation (22) for $E_0 \geqslant 2zJ$. Therefore, m is obtained from Eq. (25) as long as $2zJm > E_0$, and then switches to values obtained from Eq. (26) for smaller values of m. This leads to a discontinuity in the derivative of m with respect to T at the value of T for which $2zJm = E_0$. The transition temperature is $2zJ$ for *all* positive values of E_0 and the transition is continuous, similar to the equilibrium transition for $E_0 = 0$.

The behavior for $E_0 < 0$ is quite different. We consider values of E_0 in the range $0 < |E_0| < 2zJ$ because there is no transition for $|E_0| \geqslant 2zJ$. For such values of E_0, the transition probabilities in Eq. (18) take the following forms for $m > 0$:

$$W_{+1\to-1} = \begin{cases} e^{-\beta[2zJm-|E_0|]}, & 2zJm - |E_0| > 0, \\ 1, & 2zJm - |E_0| \leqslant 0, \end{cases} \tag{27}$$

$$W_{-1\to+1} = 1. \tag{28}$$

It is clear from Eqs. (27) and (28) that both $W_{+1\to-1}$ and $W_{-1\to+11}$ are equal to 1 for $m \leqslant |E_0|/(2zJ)$. Thus there is no self-consistent solution for nonzero m with $m \leqslant |E_0|/(2zJ)$. The self-consistent solution for $m > |E_0|/(2zJ)$ is

$$m(2zJm > |E_0|) = \tanh[\beta(Jzm - |E_0|/2)]. \tag{29}$$

This equation admits a physical solution with $m > |E_0|/(2zJ)$ for temperatures less than T^* that is determined from the implicit equation

$$\sqrt{1 - k_BT^*/(Jz)} = \tanh\{[Jz\sqrt{1 - k_BT^*/(Jz)} - |E_0|/2]/(k_BT^*)\}, \tag{30}$$

which results from the condition of stability of the fixed point solution of Eq. (29). Thus MF theory for negative values of E_0 with $|E_0| < 2zJ$ predicts a *first order* transition at the temperature T^* that decreases as $|E_0|$ is increased and goes to zero for $|E_0| = 2zJ$.

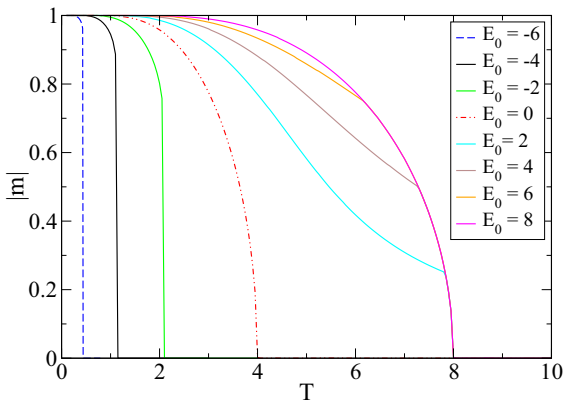

FIG. 1. Magnetization $|m|$ in MF theory vs temperature T for various values of E_0 for Metropolis dynamics.

For the Glauber algorithm, Eq. (14) with the MF approximation of Eq. (17) gives

$$r(\beta, m, E_0) = \frac{1 + e^{\beta(-2zJm+E_0)}}{1 + e^{\beta(2zJm+E_0)}}, \tag{31}$$

and therefore, from Eq. (20), we obtain

$$m = \frac{e^{2\beta zJm} - e^{-2\beta zJm}}{2\,e^{-\beta E_0} + e^{2\beta zJm} + e^{-2\beta zJm}} = \frac{\sinh[2\beta zJm]}{e^{-\beta E_0} + \cosh[2\beta zJm]}. \tag{32}$$

For $E_0 \to \pm\infty$ where DBC holds, this equation gives $m = \tanh[2\beta zJm]$ for $E_0 \to \infty$ and $m = 0$ for $E_0 \to -\infty$. Similarly for $E_0 = 0$, Eq. (32) yields $m(E_0 = 0) = \tanh[\beta zJm]$. Thus, when the DBC is satisfied, both Glauber and Metropolis algorithms yield the same self-consistency equations for the MF magnetization m and therefore the same $T_c^{\rm MF}$. For other values of E_0, Eq. (32) predicts a continuous transition similar to that in the equilibrium model. This would mean that, for general nonzero values of E_0, MF theory predicts very different behavior for Metropolis and Glauber update rules. This is not surprising because these two update rules are guaranteed to lead to the same (equilibrium) distribution in the long time limit only when DBC is satisfied. Since DBC is not satisfied for a general nonzero value of E_0, the two algorithms can lead to steady states with different statistical properties.

Results obtained from numerical solutions of the MF equations for a square lattice with $z = 4$ are shown in Fig. 1 and Fig. 2. Figure 1 shows plots of the MF magnetization $|m|$ in the Metropolis algorithm as a function of temperature T (in units of J/k_B) for various values of E_0 (in units of J). For $E_0 = 0$, the MF critical temperature is $T_c^{\rm MF} = 4$ as expected.

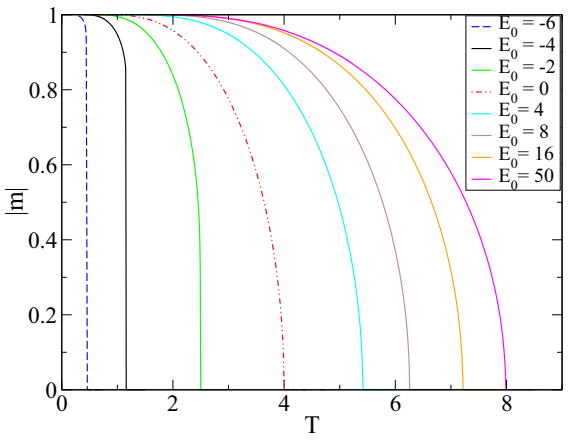

FIG. 2. Magnetization $|m|$ in MF theory vs temperature T for various values of E_0 for Glauber dynamics.

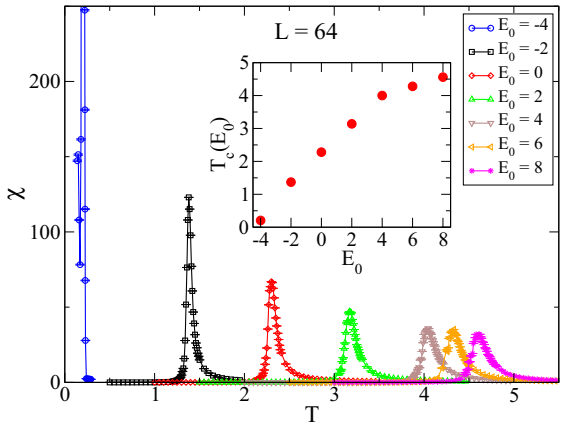

FIG. 3. Plot of susceptibility $\chi(E_0, T)$ as a function of temperature T for $L = 64$ with varying E_0 (see keys). The position of a peak gives an estimate of $T_c(E_0)$. The inset is a plot of $T_c(E_0)$ vs E_0.

For $E_0 < 0$, a first order transition takes place at $T^*(E_0)$ that decreases with decreasing E_0 and goes to zero as $E_0 \to -8$. For $E_0 > 0$, the magnetization curves of $E_0 < 8$ coincide with the magnetization curve for $E_0 = 8$ at $m = E_0/8$, and then follow $m(E_0 = 8, T)$ for all $m < E_0/8$. Thus, for $E_0 > 0$, $T_c^{\rm MF}$ in the Metropolis dynamics is 8.

Figure 2 shows plots of the MF magnetization in the Glauber dynamics as a function of T for various values of E_0. At $E_0 = 0$, $T_c^{\rm MF} = 4$. For $E_0 > 0$, $T_c^{\rm MF}$ increases with increasing E_0 and approaches 8 for very large values of E_0. For $E_0 < 0$, $T_c^{\rm MF}$ decreases with decreasing E_0, and goes to 0 as $E_0 \to -\infty$.

V. DETAILED NUMERICAL RESULTS

In this section, we present the results of Monte Carlo simulations of the model for different values of E_0 using the Metropolis algorithm. We calculate physical quantities such as the magnetization per spin m, the Binder-cumulant U_4 associated with the distribution of the magnetization, the specific-heat per spin c (in units of k_B), and the magnetic susceptibility χ (in units of $1/J$). These quantities are defined as

$$m(T, L) = \langle \widehat{m} \rangle, \quad \widehat{m} = \frac{1}{N} \sum_i s_i, \tag{33}$$

$$U_4(T, L) = 1 - \frac{\langle \widehat{m}^4 \rangle}{3 \langle \widehat{m}^2 \rangle^2}, \tag{34}$$

$$c(T, L) = \frac{1}{NT^2} \big(\langle E^2 \rangle - \langle E \rangle^2 \big), \tag{35}$$

$$\chi(T, L) = \frac{1}{NT} \big(\langle M^2 \rangle - \langle M \rangle^2 \big), \tag{36}$$

where N is the number of spins, $\langle \cdots \rangle$ denotes an average in the steady state at a temperature T, $E = -\sum_{<ij>} s_i s_j$ is the total energy, and $M = N\widehat{m}$. Note that we have defined the specific heat and the susceptibility in terms of correlation functions, in the same way as these quantities are defined in an equilibrium system. However, in our nonequilibrium system, these quantities *do not* satisfy the usual relations with response functions (the derivative of the energy with respect to T for the specific heat and the derivative of the magnetization with respect to a magnetic field for the susceptibility) that are satisfied in a system in thermal equilibrium.

We use finite-size scaling (FSS) to analyze the dependence of these quantities on the system size $N = L^2$. We assume that the FSS forms for these quantities are the same as those for a system in thermal equilibrium:

$$m(T, L) = L^{-\beta/\nu} \mathcal{M}((T - T_c) L^{1/\nu}), \tag{37}$$

$$U_4(T, L) = \mathcal{U}((T - T_c) L^{1/\nu}), \tag{38}$$

$$c(T, L) = L^{\alpha/\nu} \mathcal{C}((T - T_c) L^{1/\nu}), \tag{39}$$

$$\chi(T, L) = L^{\gamma/\nu} \mathcal{X}((T - T_c) L^{1/\nu}), \tag{40}$$

where $\mathcal{M}, \mathcal{U}, \mathcal{C}, \mathcal{X}$ are the scaling functions and α, β, γ and ν are the critical exponents for specific heat, magnetization, susceptibility, and correlation length, respectively. As described below, our results for these quantities satisfy these FSS forms within the accuracy of our numerical computation.

To begin with, we present in Fig. 3 the plots of $\chi(E_0, T)$ as a function of T for $L = 64$ and various values of E_0 to show qualitatively the dependence of the transition temperature T_c on E_0. The peak positions of χ give estimates of $T_c(E_0)$. Notice the shifting of T_c to higher values with increasing E_0. The inset of this figure shows a plot of $T_c(E_0)$, estimated as the value of T at which $\chi(E_0, T)$ peaks, as a function of E_0. For $E_0 = 0$, the model has an equilibrium phase transition at $T_c(E_0 = 0) \simeq 2.269$. It is clear from the plot in the inset that T_c approaches zero for large negative values of E_0 and it is $\simeq 2T_c(E_0 = 0)$ for $E_0 = 8$. This is in agreement with the results in Sec. III. We now study the nature of the nonequilibrium transitions for nonzero values of E_0 in the range $-8 < E_0 < 8$. For a detailed numerical study, we choose $E_0 = \pm 2$ and perform large-scale MC simulations only for these two values of E_0.

A. Numerical results for $E_0 = -2J$

We start with a demonstration of the nonequilibrium nature of the model for $E_0 \neq 0$. In an equilibrium system, the specific heat defined as the derivative of the internal energy $\langle E \rangle$ with respect to the temperature T, i.e., $C = d\langle E \rangle / dT$, is exactly the same as the specific heat obtained from energy fluctuations

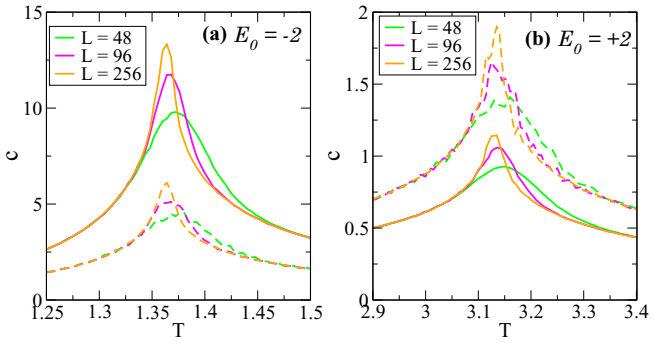

FIG. 4. Plot of the specific heat per spin $c = 1/(NT^2)(\langle E^2\rangle - \langle E\rangle^2)$ (shown by the solid curves) and the derivative of the energy with respect to temperature, $N^{-1}d\langle E\rangle/dT$ (shown by the dashed curves), for (a) $E_0 = -2$ and (b) $E_0 = +2$. Numerically, the derivative is calculated using first-order finite difference and it is taken at the midpoint of the interval instead of either end point. Results are shown for three values of L. Data for same L are plotted with the same color.

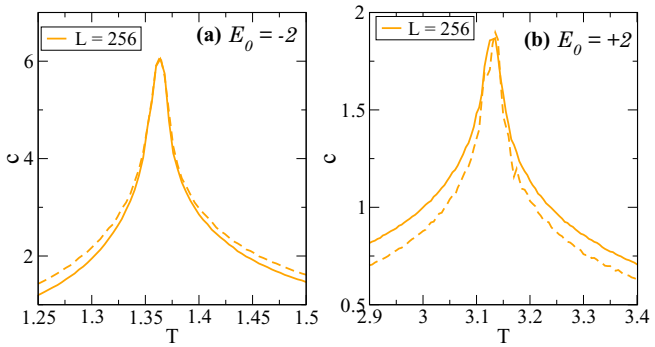

FIG. 5. Plot of $N^{-1}d\langle E\rangle/dT$ (shown by the dashed curves) and $\epsilon/(NT^2)(\langle E^2\rangle - \langle E\rangle^2)$ (shown by the solid curves) for (a) $E_0 = -2$ and (b) $E_0 = +2$. The ϵ value is 0.454 for $E_0 = -2$ and 1.632 for $E_0 = +2$. Data are shown only for the largest $L = 256$.

[Eq. (35)], i.e.,

$$\frac{d\langle E\rangle}{dT} = \frac{1}{T^2}(\langle E^2\rangle - \langle E\rangle^2). \tag{41}$$

This relation does not hold for a nonequilibrium system. As shown in panel (a) of Fig. 4, this relation is not satisfied for $E_0 = -2$. In this figure, the solid curves represent the specific heat per spin from energy fluctuations and the dotted curves represent the derivative $1/Nd\langle E\rangle/dT$ (the derivative is calculated from first-order finite difference). The difference between the solid and dashed curves for each value of L is strong evidence for the nonequilibrium nature of the system.

To establish conclusively the nonequilibrium nature of the model, it is also necessary to show that the difference between the two curves corresponding to the two definitions of the specific heat cannot be removed by scaling one of the curves by a constant numerical factor ϵ. If this were the case, then the factor ϵ could be absorbed by simply scaling the temperature by the same factor. To check this possibility, we have chosen the value of ϵ for which the heights of the peaks of the two curves coincide. Plots of ϵc and $N^{-1}d\langle E\rangle/dT$ for this choice of ϵ are shown in panel (a) of Fig. 5 for the largest value of L (=256) considered. Clearly, the two curves move away from each other as the temperature is changed from the value at the peak. This confirms the nonequilibrium nature of the system for $E_0 = -2$. Similarly the panels (b) of Figs. 4 and 5 show the nonequilibrium nature of the system for $E_0 = +2$, the case which we discuss later.

Having established the nonequilibrium nature of the transition for $E_0 = -2$, we now proceed to use FSS to examine the critical behavior. Figure 6 shows a plot of the Binder cumulant $U_4(T, L)$ as a function of T for various values of L. From the FSS relation for $U_4(T, L)$ [Eq. (38)], it is clear that U_4 for different L converge to the same value as $T \to T_c$. In Fig. 6, the cumulant curves for different L intersect at a point and this intersection point gives an estimate of the critical temperature, $T_c \simeq 1.36$.

Next, in Fig. 7(a), we show a plot of the specific heat per spin (c) vs temperature T for various values of L. In Fig. 7(b), we plot the susceptibility (χ) vs temperature T for various values of L. The specific heat c shows a peak at an L-dependent pseudocritical temperature $T^*(L)$ which shifts to smaller values with increasing L, and the height of the peak grows with increasing L. To obtain the location and the height of the peak at a particular value of L, we fit the data near the peak with a parabolic function $y = a(x - x_0)^2 + h$, where x_0 gives the position of the peak $T^*(L)$ and h gives the height of the peak $c^{\max}(L)$. Similarly χ also shows peaks which shift to lower T with increasing L. If the FSS function $\mathcal{C}(x)$ or $\mathcal{X}(x)$ in Eqs. (39) and (40) peaks at some value, say x_0, then the peak position $T^*(L)$ for a particular value of L varies with L as

$$T^*(L) = T_c + x_0 L^{-1/\nu}, \tag{42}$$

and the maximum value of the *singular* part of c, χ in a finite size system varies as

$$c^{\max} \propto L^{\alpha/\nu} \tag{43}$$

and

$$\chi^{\max} \propto L^{\gamma/\nu}. \tag{44}$$

Figure 8 shows a plot of $c^{\max}(L)$ vs L in a double-logarithmic scale, where one can clearly see the negative curvature in the data points. This indicates that $c^{\max}(L)$ has a

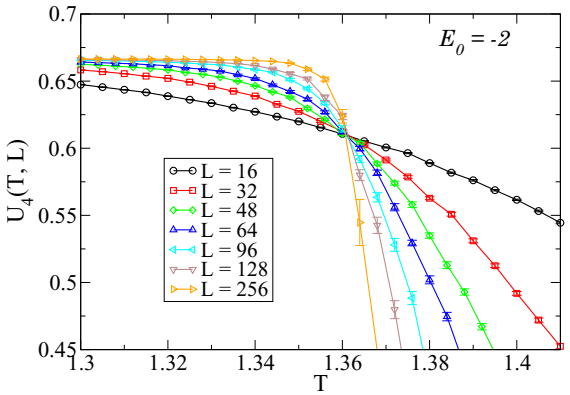

FIG. 6. Binder cumulant $U_4(T, L)$ for different values of L vs temperature T for $E_0 = -2$. The intersection point for different values of L gives the critical temperature $T_c \simeq 1.36$.

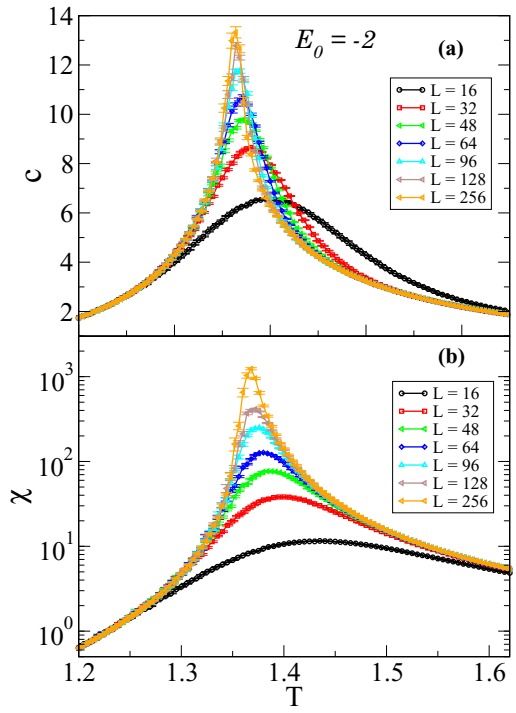

FIG. 7. (a) Specific-heat per spin $c(T, L)$ vs temperature T for $E_0 = -2$. (b) Susceptibility $\chi(T, L)$ vs temperature T on a log-linear scale for $E_0 = -2$.

weaker than power-law dependence on L. Therefore, expecting $\alpha = 0$, as in the equilibrium two-dimensional Ising model, we plot $c^{\max}(L)$ on a semilog scale in the inset of Fig. 8, where the L axis is logarithmically scaled. Here a linear behavior is clearly visible with no curvature and a straight line is the best fit to the behavior,

$$c^{\max}(L) = A + B \ln L, \tag{45}$$

where A is the *regular* part of the specific heat. The logarithmic divergence of $c^{\max}(L)$ implies that $\alpha = 0$.

Next, in Fig. 9, we plot $\chi^{\max}(L)$ vs L in a double-logarithmic scale. Here we can clearly observe a linear

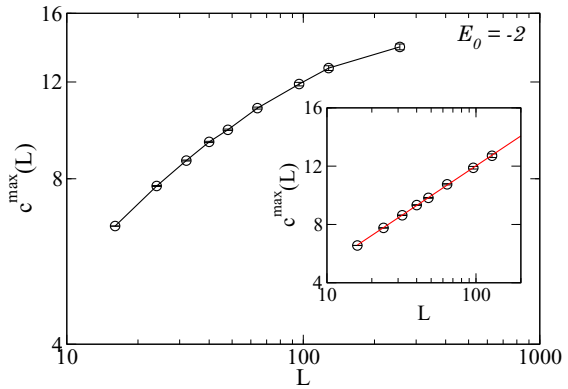

FIG. 8. Maximum value of the specific heat per spin $c^{\max}(L)$ vs L in a log-log plot. The inset shows the same data in a semilog scale. The red solid line shows the best fit to the function $A + B \ln L$ with $A = -1.63$ and $B = 2.96$.

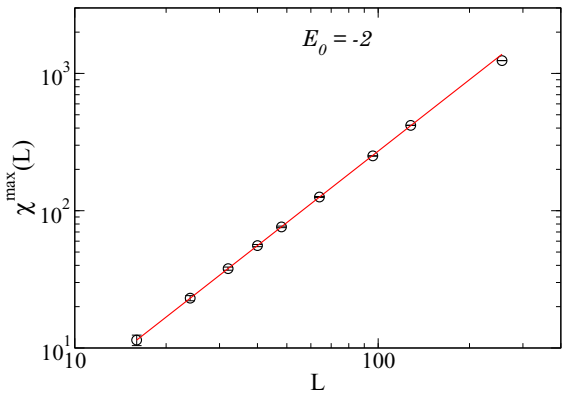

FIG. 9. Maximum value of the susceptibility $\chi^{\max}(L)$ vs L in a log-log scale. The red solid line is the best fit to the form $AL^{\gamma/\nu}$ with $A = 0.095$ and $\gamma/\nu = 1.73 \pm 0.01$.

behavior which agrees with the power-law form of $\chi^{\max}(L)$ given in Eq. (44). The solid line is the best power-law fit that gives $\gamma/\nu = 1.73 \pm 0.01$.

In Fig. 10, we show plots of the peak positions of c and χ, i.e., the pseudocritical points $T^*(L)$ as a function of L^{-1}, marked by the point symbols. We jointly fit this data to the function $y = a_0 + a_1 x^{a_2}$ suggested in Eq. (42) with the common values of a_0 and a_2, where a_0 gives T_c and a_2 gives $1/\nu$. The two solid lines in red are the result of the best joint fit to this function for c and χ. The quality of fit is very high, with a value of goodness-of-fit parameter $Q = 0.9$, and produces the estimates $1/\nu = 0.98 \pm 0.03$ and $T_c = 1.3604 \pm 0.0003$. Figure 11 shows the scaling of χ by plotting $\chi L^{-\gamma/\nu}$ against $[T - T^*(L)]L^{1/\nu}$. Clearly, the data collapse is excellent. The exponent values used here are $\gamma/\nu = 1.73$ and $1/\nu = 0.98$.

Figure 12 shows a plot of the absolute value of the magnetization per spin $|m|$ as a function of T for various values of L. As suggested in the FSS of the magnetization, Eq. (37), we plot $mL^{\beta/\nu}$ vs $(T - T_c)L^{1/\nu}$ and obtain the critical exponents β/ν that give the best scaling collapse, using the values of

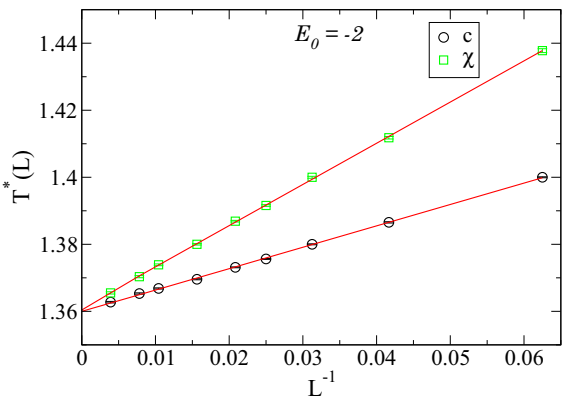

FIG. 10. Plot of pseudocritical points $T^*(L)$ where c and χ attain their maxima. The black and green symbols are the peak positions of c and χ, respectively. The red lines are the best simultaneous fit of the form Eq. (42), in which the values of T_c and $1/\nu$ are shared during the fitting procedure. This fit yields $T_c = 1.3604 \pm 0.0003$ and $1/\nu = 0.98 \pm 0.03$.

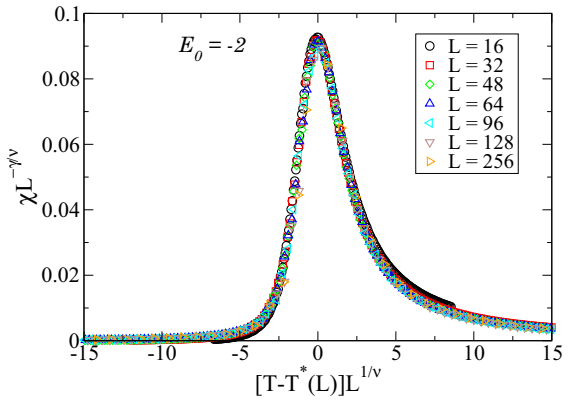

FIG. 11. FSS of the susceptibility: plot of $\chi L^{-\gamma/\nu}$ vs $[T - T^*(L)]L^{1/\nu}$ with $\gamma/\nu = 1.73$ and $1/\nu = 0.98$.

T_c and $1/\nu$ estimated above. This FSS data collapse of the magnetization is shown in Fig. 13. The value of exponent β/ν obtained from this FSS analysis is 0.123 ± 0.005. All calculated exponents are tabulated in Table I, showing all critical exponents α, β/ν, γ/ν, and $1/\nu$ for $E_0 = -2$ to be consistent with those for $E_0 = 0$, i.e., the case of an equilibrium 2D Ising model on a square lattice. However, as expected, the critical temperature is reduced from $T_c = 2.269$ for $E_0 = 0$ to $T_c \simeq 1.36$ for $E_0 = -2$.

This value of T_c can be understood from the following argument. As in the equilibrium Ising model on a square lattice, ΔE in our model can take a value from the set $\{-8, -4, 0, 8, 4\}$ in units of J. With positive ΔE, from Eqs. (7) and (9), $W_{s_i \to -s_i} = e^{-\beta(\Delta E - 2)}$ and $W_{-s_i \to s_i} = 1$, and thus the ratio of these two transition probabilities is $e^{-\beta(\Delta E - 2)}$. Equating this with the ratio of transition probabilities for the equilibrium system ($E_0 = 0$) at temperature $T^0 = 1/\beta^0$, we get

$$\beta^0 \Delta E = \beta(\Delta E - 2). \tag{46}$$

Similarly for $\Delta E < 0$, we get

$$\beta^0 |\Delta E| = \beta(|\Delta E| - 2). \tag{47}$$

These equations allow us to relate T to a temperature T^0 of the equilibrium Ising model. Since this relation is different for

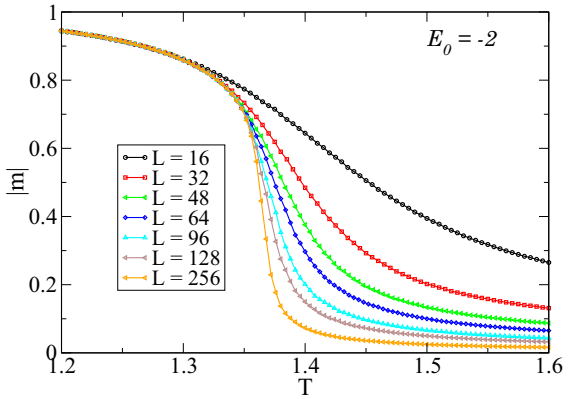

FIG. 12. Absolute value of the magnetization per spin $m(T, L)$ vs temperature T for $E_0 = -2$. The data are shown for various L values.

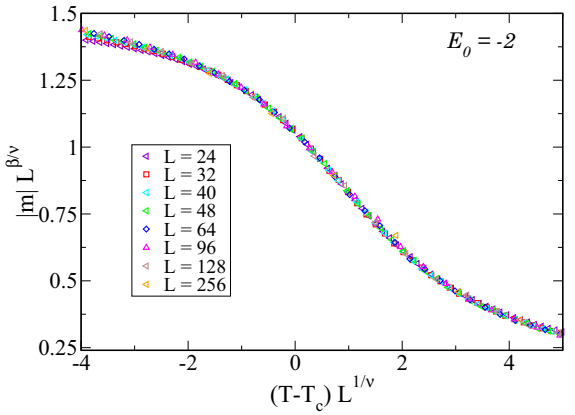

FIG. 13. Finite size scaling of the magnetization data by plotting $mL^{\beta/\nu}$ vs $(T - T_c)L^{1/\nu}$. The exponent value from the best data collapse is $\beta/\nu = 0.123 \pm 0.005$, after using our estimates for $1/\nu = 0.98$, and $T_c = 1.3604$.

different values of ΔE, it is not possible to map the probability distribution in the steady state of our model to the equilibrium distribution at a unique temperature T^0. This, again, confirms the nonequilibrium nature of our model for $E_0 \neq 0$. At the critical point, Eqs. (46) and (47) imply $\beta_c(|\Delta E| - 2) = \beta_c^0 |\Delta E|$, where $\beta_c^0 = 1/T_c^0$, with $T_c^0 = 2.269$ being the critical temperature of the equilibrium Ising model on a square lattice. This gives $T_c = 1.135$ if we take $|\Delta E| = 4$ and $T_c = 1.702$ for $|\Delta E| = 8$.

To get an approximate unique value for T_c, it is necessary to average over the different values of T_c obtained for different choices for ΔE. The Ising model Hamiltonian in terms of ΔE can be written as

$$\mathcal{H} = -\frac{1}{4} \sum_i \Delta E(s_i \to -s_i). \tag{48}$$

Thus the equilibrium average, $\langle \Delta E \rangle$, of ΔE is equal to $-4\langle E \rangle/N$. From the exact solution of the 2D Ising model [65–67], the energy per spin $\langle E \rangle/N$ at the critical point (T_c^0) is equal to $-\sqrt{2}$, which means at criticality, $\langle \Delta E \rangle \sim 4\sqrt{2}$. Then, from Eq. (46), we get

$$T_c(E_0 = -2) \sim T_c^0 \left(1 - \frac{2}{4\sqrt{2}}\right) = 1.467. \tag{49}$$

TABLE I. Summary of the values of the critical temperature T_c, and the critical exponents α, β/ν, γ/ν, and $1/\nu$ for $E_0 = \pm 2$ obtained from FSS. We also show the known values of these exponents for $E_0 = 0$ for reference. The numbers in parentheses are error estimates for the last significant digits.

	T_c	α	β/ν	γ/ν	$1/\nu$
$E_0 = 0$ (known results)	2.269	0	0.125	1.75	1
$E_0 = 2$ (This work)	3.1267(4)	0	0.122(5)	1.72(3)	0.97(3)
$E_0 = -2$ (This work)	1.3604(3)	0	0.123(5)	1.73(1)	0.98(3)

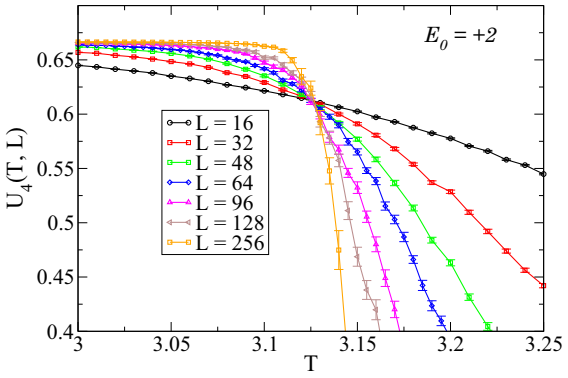

FIG. 14. Binder cumulant $U_4(T, L)$ vs temperature T for $E_0 = 2$. The intersection point for various values of L gives the critical temperature $T_c \simeq 3.127$.

This approximate estimate of $T_c \sim 1.467$ is close to the value, $T_c \simeq 1.36$, obtained from our simulations. The difference arises from considering $\langle \Delta E \rangle$ instead of the average of $1/\Delta E$, and neglecting the possibility of having $\Delta E = 0$, etc., in the calculation of T_c.

B. Numerical results for $E_0 = +2J$

We now present the numerical results for $E_0 = 2J$. The nonequilibrium nature of the model for $E_0 = +2$ has already been established in panel (b) of Figs. 4 and 5. To examine the critical behavior, let us start to get an estimate of T_c by plotting $U_4(T, L)$ vs T, which are shown in Fig. 14. These U_4 curves intersect at a point and predict $T_c \simeq 3.127$. The specific-heat c and susceptibility χ show peaks that are shifted towards lower T with increasing L (data not shown). The finite-size behavior of the peak heights $c^{\max}(L)$, $\chi^{\max}(L)$ is similar to that found for $E_0 = -2$, as shown in Fig. 15, which confirms a logarithmic divergence of $c^{\max}$ with $\alpha = 0$ and a power-law divergence of $\chi^{\max}(L)$ with $\gamma/\nu = 1.72 \pm 0.03$.

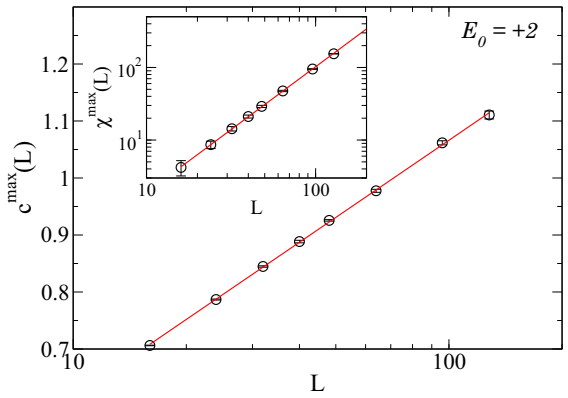

FIG. 15. Maximum of the specific heat per spin $c^{\max}(L)$ vs L on a semilog scale. The red solid line shows the best fit to the function $A + B \ln L$ with $A = 0.17$ and $B = 0.195$. The inset shows the maximum of the susceptibility $\chi^{\max}(L)$ vs L on a log-log scale. Here the red solid line is the best fit to the form $AL^{\gamma/\nu}$ with $A = 0.037 \pm 0.005$ and $\gamma/\nu = 1.72 \pm 0.03$.

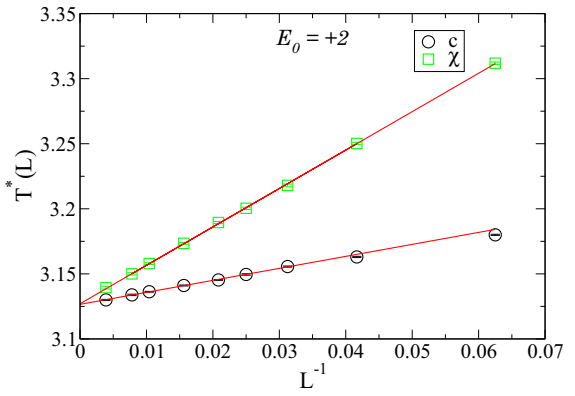

FIG. 16. Plot of the pseudocritical temperature $T^*(L)$ where c and χ attain their maxima. The black and green symbols are the peak positions of c and χ, respectively. The red lines are the simultaneous fit of the form Eq. (42), which yield $T_c = 3.1267 \pm 0.0004$, and $1/\nu = 0.973 \pm 0.028$.

In Fig. 16, the pseudocritical temperatures $T^*(L)$ obtained from the specific heat and the susceptibility are plotted in point symbols as functions of L^{-1}. Again, we perform a joint fit to the function of the form of Eq. (42), where the values of T_c and $1/\nu$ are shared in the fit. The two solid lines show the result of this joint fit that gives $1/\nu = 0.973 \pm 0.028$, and $T_c = 3.1267 \pm 0.0004$ with the value of goodness-of-fit parameter $Q = 0.7$, which is very high. Figure 17 shows the best data collapse for χ in a plot of $\chi L^{-\gamma/\nu}$ against $[T - T^*(L)]L^{1/\nu}$. The exponent values corresponding to the best scaling collapse are $\gamma/\nu = 1.72$ and $1/\nu = 0.97$. Figure 18 shows a scaling plot for the magnetization, where the best data collapse after using the above estimated values for T_c and $1/\nu$ gives $\beta/\nu = 0.122 \pm 0.005$. Arguments identical to those for $E_0 = -2$ yield the following estimate for the critical temperature:

$$T_c(E_0 = +2) = T_c^0\left(1 + \frac{2}{|\Delta E|}\right)$$
$$\simeq T_c^0\left(1 + \frac{2}{4\sqrt{2}}\right) = 3.071. \qquad (50)$$

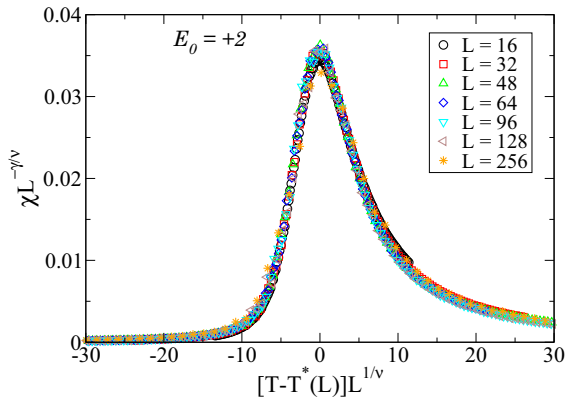

FIG. 17. FSS of the susceptibility: plot of $\chi L^{-\gamma/\nu}$ vs $[T - T^*(L)]L^{1/\nu}$ with $\gamma/\nu = 1.72$ and $1/\nu = 0.97$.

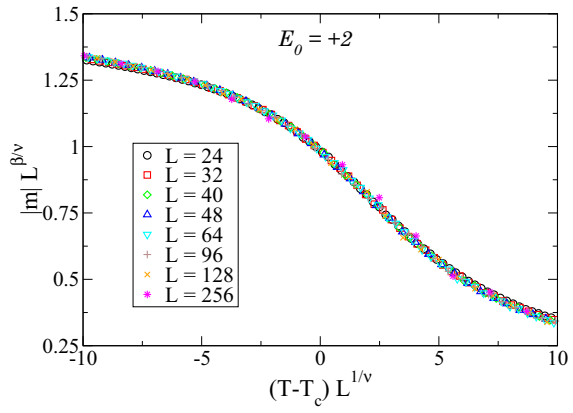

FIG. 18. FSS of the magnetization: $mL^{\beta/\nu}$ is plotted vs $(T - T_c)L^{1/\nu}$. The exponent value from the best data collapse is $\beta/\nu = 0.122 \pm 0.005$, after using previous estimates of $1/\nu = 0.97(3)$ and $T_c = 3.1267$ for $E_0 = +2$.

This estimate is close to the value, $T_c \simeq 3.127$, obtained from simulations.

The final results for the critical temperature and all exponents are listed in Table I. For both $E_0 = -2$ and $E_0 = +2$, all the critical exponents α, β/ν, γ/ν, and $1/\nu$ are found to be consistent with those for the equilibrium Ising model ($E_0 = 0$), which establishes that our nonequilibrium model falls in the Ising universality class. This is in line with the several other nonequilibrium models that do not obey DBC [8,25,26,68–74].

VI. SUMMARY AND DISCUSSION

We have studied the nature of the phase transition and critical behavior of a nonequilibrium Ising model in $d = 2$, where modified versions of the Metropolis and Glauber dynamics, which do not satisfy the DBC, are used to update the spins. The violation of DBC in the model is characterized by nonzero values of a parameter E_0. For $E_0 \neq 0$, the system reaches the nonequilibrium steady states which are not described by Boltzmann statistics. We presented the results of a MF theory that predicts interesting phase behavior for $E_0 \neq 0$. We find that the predicted phase diagrams for (modified) Metropolis and (modified) Glauber dynamics are quite different. In the former case, we find a first order phase transition for $E_0 < 0$ and a continuous phase transition for $E_0 > 0$ that takes place at the same temperature for different values of E_0. In the latter case, we find a continuous phase transition for both positive and negative values of E_0 at a temperature that increases continuously with E_0. This strong dependence on the microscopic dynamics is unusual, but not entirely unexpected because the steady states reached by the system under different update rules that do not satisfy the DBC may very well be different.

We have also performed a comprehensive numerical study of the phase behavior of the model in two dimensions for $E_0 = \pm 2$ via MC simulations using the modified Metropolis dynamics. We calculated physical quantities such as magnetization, Binder cumulant, specific heat (obtained from energy fluctuations), and susceptibility (obtained from fluctuations of the magnetization), and carried out a FSS analysis. The critical exponents for both values of E_0, summarized in Table I, are found to be consistent with those of the equilibrium case. Thus, contrary to the predictions of MF theory, the phase transition in the nonequilibrium model in two dimensions appears to be in the same universality class as that of the equilibrium Ising model. This is in agreement with previous studies [8,23–26,69–75], which have shown that the critical properties of the nonequilibrium systems considered there fall in the universality class of the equilibrium Ising model. However, in nonequilibrium driven diffusive systems (e.g., lattice gas) of attractive (ferromagnetic) interparticle interaction [9,14,76–78] and reaction-diffusion systems [13,16], etc., the critical behavior is found to be in the different universality classes.

An interesting question in this context is whether the nonequilibrium model for $E_0 \neq 0$ has an upper critical dimension d_u such that the critical behavior is described by MF theory for physical dimensions higher than d_u. In most equilibrium systems, one finds that the behavior for $d < d_u$ is more complex than that for $d > d_u$, whereas the opposite seems to be true for the nonequilibrium model with Metropolis dynamics considered here. The prediction of MF theory is particularly different from simulation results for $E_0 < 0$ for which MF theory predicts a strong first order transition, but simulations show a continuous transition. This is unusual in equilibrium systems, although some examples of similar behavior do exist. For example, MF theory predicts a first order transition for the three-state Potts model, but it exhibits a continuous transition in two dimensions [79]. Another possibility that we cannot rule out is that the first-order transition found for $E_0 < 0$ in the MF theory is an artifact of the single-site approximation and a more sophisticated MF treatment could lead to a continuous phase transition.

Another interesting direction is to study the dynamical properties of such models that violate DBC. In the literature [80–86], several Markov-chain Monte Carlo (MCMC) methods without DBC (often also called nonreversible or irreversible algorithms) have been proposed which are shown to make the relaxation towards the target steady state very fast and to reduce the effect of critical slowing down. However, these methods still satisfy the global balance, only locally the DBC is violated, which is not the case in our model for $E_0 \neq 0$. Also, it is not well understood how the irreversible MCMC methods affect the dynamical critical exponent. Therefore, further work in this direction would be useful.

ACKNOWLEDGMENTS

The authors thank M. Weigel (Coventry University, UK) for critically reading the manuscript and providing very useful feedback in order to improve the content of the paper. Numerical results were obtained using the *Mario* Computing Cluster at ICTS, Bengaluru. M.K. would like to acknowledge the support of an ICTS postdoctoral fellowship and the Royal Society–SERB Newton International fellowship (No. NIF/R1/180386).

[1] N. Goldenfeld, *Lectures on Phase Transitions and The Renormalization Group* (CRC Press, Boca Raton, FL, 2018).
[2] R. Stinchcombe, Adv. Phys. **50**, 431 (2001).
[3] Z. Rácz, in *Slow Relaxations and Nonequilibrium Dynamics in Condensed Matter*, edited by J.-L. Barrat, M. V. Feigelman, J. Kurchan, and J. Dalibard (Springer, New York, 2003), pp. 1–40.
[4] D. Mukamel, in *Soft and Fragile Matter: Nonequilibrium Dynamics, Metastability and Flow*, edited by M. E. Cates and M. R. Evans (CRC Press, Boca Raton, FL, 2000), p. 237.
[5] G. Ódor, Rev. Mod. Phys. **76**, 663 (2004).
[6] B. Schmittmann and R. Zia, in *Statistical Mechanics of Driven Diffusive System*, Phase Transitions and Critical Phenomena Vol. 17, edited by C. Domb and J. L. Lebowitz (Academic Press, New York, 1995), pp. 3–214.
[7] B. Schmittmann and R. Zia, Phys. Rep. **301**, 45 (1998).
[8] K.-t. Leung, B. Schmittmann, and R. K. P. Zia, Phys. Rev. Lett. **62**, 1772 (1989).
[9] B. Schmittmann, Int. J. Mod. Phys. B **04**, 2269 (1990).
[10] K.-t. Leung and J. L. Cardy, J. Stat. Phys. **44**, 567 (1986); H. Janssen and B. Schmittmann, Z. Phys. B **64**, 503 (1986); K.-t. Leung, Phys. Rev. Lett. **66**, 453 (1991).
[11] H. van Beijeren and L. S. Schulman, Phys. Rev. Lett. **53**, 806 (1984).
[12] J. Marro, J. Lebowitz, H. Spohn, and M. H. Kalos, J. Stat. Phys. **38**, 725 (1985).
[13] J. Marro, J. L. Vallés, and J. M. González-Miranda, Phys. Rev. B **35**, 3372 (1987).
[14] J. Vallés and J. Marro, J. Stat. Phys. **49**, 89 (1987).
[15] S. Katz, J. L. Lebowitz, and H. Spohn, Phys. Rev. B **28**, 1655 (1983) J. Stat. Phys. **34**, 497 (1984).
[16] J.-S. Wang, K. Binder, and J. L. Lebowitz, J. Stat. Phys. **56**, 783 (1989).
[17] P. L. Garrido, J. Marro, and R. Dickman, Ann. Phys. (NY) **199**, 366 (1990); J. Marro, A. Achahbar, P. L. Garrido, and J. J. Alonso, Phys. Rev. E **53**, 6038 (1996); P. L. Garrido and J. Marro, Physica A **279**, 143 (2000).
[18] J. V. Andersen and O. G. Mouritsen, Phys. Rev. Lett. **65**, 440 (1990).
[19] J. M. Gonzalez-Miranda, P. L. Garido, J. Marro, and J. L. Lebowitz, Phys. Rev. Lett. **59**, 1934 (1987).
[20] R. Dickman, Phys. Lett. A **122**, 463 (1987).
[21] A. Szolnoki, Phys. Rev. E **62**, 7466 (2000).
[22] T. Tomé and M. J. de Oliveira, Phys. Rev. A **40**, 6643 (1989).
[23] T. Tome, M. De Oliveira, and M. Santos, J. Phys. A: Math. Gen. **24**, 3677 (1991).
[24] M. Marques, Phys. Lett. A **145**, 379 (1990); J. Phys. A: Math. Gen. **22**, 4493 (1989).
[25] M. Godoy and W. Figueiredo, Phys. Rev. E **65**, 026111 (2002); **61**, 218 (2000).
[26] W. Figueiredo and B. C. Grandi, Braz. J. Phys. **30**, 58 (2000).
[27] P. L. Garrido, J. Marro, and J. M. González-Miranda, Phys. Rev. A **40**, 5802 (1989).
[28] P. Garrido, A. Labarta, and J. Marro, J. Stat. Phys. **49**, 551 (1987).
[29] T. Halpin-Healy and Y.-C. Zhang, Phys. Rep. **254**, 215 (1995).
[30] A.-L. Barabási and H. E. Stanley, *Fractal Concepts in Surface Growth* (Cambridge University Press, Cambridge, UK, 1995).
[31] J. Krug and H. Spohn, Phys. Rev. A **38**, 4271 (1988).
[32] M. Kardar, G. Parisi, and Y.-C. Zhang, Phys. Rev. Lett. **56**, 889 (1986); F. Family, Physica A **168**, 561 (1990).
[33] J. Marro and R. Dickman, *Nonequilibrium Phase Transitions in Lattice Models* (Cambridge University Press, Cambridge, UK, 2005).
[34] H.-K. Janssen, Z. Phys. B **42**, 151 (1981).
[35] F. Schlögl, Z. Phys. **253**, 147 (1972).
[36] M. Katori and N. Konno, J. Magn. Magn. Mater. **104-107**, 267 (1992).
[37] H. Hinrichsen, Adv. Phys. **49**, 815 (2000).
[38] M. C. Marchetti, J. F. Joanny, S. Ramaswamy, T. B. Liverpool, J. Prost, M. Rao, and R. A. Simha, Rev. Mod. Phys. **85**, 1143 (2013).
[39] E. V. Albano, Phys. Rev. Lett. **77**, 2129 (1996).
[40] T. Vicsek, A. Czirók, E. Ben-Jacob, I. Cohen, and O. Shochet, Phys. Rev. Lett. **75**, 1226 (1995).
[41] M. E. Cates and J. Tailleur, Annu. Rev. Condens. Matter Phys. **6**, 219 (2015).
[42] J. Smrek and K. Kremer, Phys. Rev. Lett. **118**, 098002 (2017).
[43] J. Smrek and K. Kremer, Entropy **20**, 520 (2018).
[44] S. Siva Nasarayya Chari, C. Dasgupta, and P. K. Maiti, Soft Matter **15**, 7275 (2019).
[45] S. N. Weber, C. A. Weber, and E. Frey, Phys. Rev. Lett. **116**, 058301 (2016).
[46] B. Trefz, J. T. Siebert, T. Speck, K. Binder, and P. Virnau, J. Chem. Phys. **146**, 074901 (2017).
[47] J. T. Siebert, F. Dittrich, F. Schmid, K. Binder, T. Speck, and P. Virnau, Phys. Rev. E **98**, 030601(R) (2018).
[48] M. Droz, A. L. Ferreira, and A. Lipowski, Phys. Rev. E **67**, 056108 (2003).
[49] A. Lipowski and M. Droz, Phys. Rev. E **65**, 056114 (2002).
[50] I. Dornic, H. Chaté, J. Chave, and H. Hinrichsen, Phys. Rev. Lett. **87**, 045701 (2001).
[51] P. Grassberger, Z. Phys. B **47**, 365 (1982).
[52] I. Jensen and R. Dickman, Phys. Rev. E **48**, 1710 (1993).
[53] I. Jensen, Phys. Rev. Lett. **70**, 1465 (1993).
[54] P. Grassberger, J. Phys. A: Math. Gen. **22**, 3673 (1989).
[55] H. Park and H. Park, Physica A **221**, 97 (1995).
[56] H. Hinrichsen, Phys. Rev. E **55**, 219 (1997).
[57] M. H. Kim and H. Park, Phys. Rev. Lett. **73**, 2579 (1994).
[58] N. Metropolis, A. W. Rosenbluth, M. N. Rosenbluth, A. H. Teller, and E. Teller, J. Chem. Phys. **21**, 1087 (1953).
[59] R. J. Glauber, J. Math. Phys. **4**, 294 (1963).
[60] W. Janke, *Computational Many-Particle Physics* (Springer, New York, 2008), pp. 79–140.
[61] M. Suzuki and R. Kubo, J. Phys. Soc. Jpn. **24**, 51 (1968).
[62] R. Zia and B. Schmittmann, J. Stat. Mech.: Theory Exp. (**2007**) P07012.
[63] O. Melchert, arXiv:0910.5403.
[64] J. A. Nelder and R. Mead, Comput. J. **7**, 308 (1965).
[65] L. Onsager, Phys. Rev. **65**, 117 (1944).
[66] G. F. Newell and E. W. Montroll, Rev. Mod. Phys. **25**, 353 (1953).
[67] B. M. McCoy and T. T. Wu, *The Two-dimensional Ising Model* (Courier Corporation, Boston, 2014).
[68] C. H. Bennett and G. Grinstein, Phys. Rev. Lett. **55**, 657 (1985); E. Domany and W. Kinzel, *ibid.* **53**, 311 (1984).
[69] G. Grinstein, C. Jayaprakash, and Y. He, Phys. Rev. Lett. **55**, 2527 (1985).
[70] U. C. Täuber, V. K. Akkineni, and J. E. Santos, Phys. Rev. Lett. **88**, 045702 (2002).

[71] M. J. de Oliveira, J. Stat. Phys. **66**, 273 (1992); M. De Oliveira, J. Mendes, and M. Santos, J. Phys. A: Math. Gen. **26**, 2317 (1993).
[72] H. Blote, J. Heringa, A. Hoogland, and R. Zia, J. Phys. A: Math. Gen. **23**, 3799 (1990).
[73] H. Blöte, J. Heringa, A. Hoogland, and R. Zia, Int. J. Mod. Phys. B **05**, 685 (1991); J. Heringa, H. Blöte, and A. Hoogland, Int. J. Mod. Phys. C **5**, 589 (1994).
[74] J.-S. Wang and J. L. Lebowitz, J. Stat. Phys. **51**, 893 (1988).
[75] K. E. Bassler and R. K. P. Zia, Phys. Rev. E **49**, 5871 (1994).
[76] B. Schmittmann and R. K. P. Zia, Phys. Rev. Lett. **66**, 357 (1991); B. Schmittmann, EPL (Europhys. Lett.) **24**, 109 (1993).
[77] E. L. Præstgaard, B. Schmittmann, and R. Zia, Eur. Phys. J. B **18**, 675 (2000); E. L. Praestgaard, H. Larsen, and R. Zia, EPL (Europhys. Lett.) **25**, 447 (1994).
[78] K. Hwang, B. Schmittmann, and R. K. P. Zia, Phys. Rev. Lett. **67**, 326 (1991); Phys. Rev. E **48**, 800 (1993).
[79] F.-Y. Wu, Rev. Mod. Phys. **54**, 235 (1982).
[80] K. S. Turitsyn, M. Chertkov, and M. Vucelja, Physica D **240**, 410 (2011).
[81] H. Suwa and S. Todo, Phys. Rev. Lett. **105**, 120603 (2010).
[82] H. C. Fernandes and M. Weigel, Comput. Phys. Commun. **182**, 1856 (2011).
[83] Y. Sakai and K. Hukushima, J. Phys. Soc. Jpn. **82**, 064003 (2013).
[84] K. Hukushima and Y. Sakai, J. Phys.: Conf. Ser. **473**, 012012 (2013).
[85] A. Ichiki and M. Ohzeki, Phys. Rev. E **88**, 020101(R) (2013).
[86] R. D. Schram and G. T. Barkema, Physica A **418**, 88 (2015).